

Temperature-driven spin reorientation transition in Fe/Mo(110) nanostructures

A. Kukunin, J. Prokop,* and H. J. Elmers

Institut für Physik, Johannes Gutenberg-Universität Mainz, Staudingerweg 7, D-55099 Mainz, Germany

(Received 24 May 2007; revised manuscript received 13 July 2007; published 18 October 2007)

Using low-temperature spin polarized scanning tunneling microscopy and spectroscopy, we observed a temperature-driven spin-reorientation transition (SRT) in Fe double layer (DL) nanostructures grown by step-flow growth on Mo(110). Magnetization components along the vertical and horizontal directions were detected with 4/16 ML Co/10 ML Au/W(110) tips with out-of-plane (4 ML Co) and in-plane (16 ML Co) magnetic sensitivities. The magnetic easy axis of the Fe DL nanostructures continuously rotates from the vertical direction at 5 K to an in-plane direction at 20 K. The rotation angle is independent of the size of the Fe DL nanostructures. Both out-of-plane and in-plane magnetic asymmetries show a strong decrease at the SRT.

DOI: [10.1103/PhysRevB.76.134414](https://doi.org/10.1103/PhysRevB.76.134414)

PACS number(s): 75.75.+a, 68.37.Ef, 75.30.Gw

I. INTRODUCTION

The spin-reorientation transition (SRT) in ferromagnetic thin films describes a change of the easy axis from the common in-plane direction to a vertical orientation, i.e., by decreasing the film thickness. Since its first experimental observation for NiFe(111)/Cu(111) films,¹ the SRT has recently attracted much scientific interest²⁻⁷ because the tailoring of perpendicular anisotropy is crucial for magnetic storage and sensor devices.⁸⁻¹⁰ The problem is complicated due to the competition of dipolar (shape) anisotropy with long-range character and short-range intrinsic anisotropies caused by the spin-orbit coupling. A spin reorientation in thin films may be caused by changing the thickness of the film,^{2,3,11,12} by adsorption of foreign atoms,¹³ by stress induced in the film,^{2,3} by film composition,¹⁴ and by temperature.^{12,15-17}

For a discussion of the SRT, it is important to consider higher-order terms of the magnetic anisotropy,¹⁸ which lead to three different types of SRT. The SRT proceeds either through a state of canted magnetization (continuous SRT) or through a state of coexisting local minima for the in-plane and vertical magnetizations (discontinuous SRT), depending on the sign of the fourth-order anisotropy contribution. The third case is the limiting case of vanishing fourth-order contribution at the transition leading to literal disappearance of anisotropy and to a loss of ferromagnetic order in two-dimensional systems.^{19,20} An anisotropy flow concept allows for a general discussion of the SRT by means of the transition trajectory set in a magnetic phase diagram built on the second- and fourth-order effective anisotropy constants.²¹

Microscopic experiments of the SRT in ultrathin films have revealed that the magnetic microstructure largely varies at the SRT^{12,15,22-25} including the occurrence of very small magnetic domains. Coexisting domains with in-plane and out-of-plane magnetizations at the SRT were first found for ultrathin Co/Au(111)/W(110) films.²⁴ In a recent publication, von Bergmann *et al.*¹⁵ investigated the coverage- and temperature-dependent SRT in the Fe double layer (DL) on W(110) using spin polarized scanning tunneling microscopy (SP-STM), finding a nanoscopic domain structure independent of temperature throughout the SRT. They also found that the temperature of the SRT increased with increasing width of the Fe DL areas.¹⁵

The magnetic microstructure at the SRT has been extensively treated theoretically for ideal structures with the restriction to second-order anisotropies.²⁶ In this case, the SRT proceeds via a broadening and coalescing of domain walls. Additional fourth-order anisotropy terms prevent the domain wall from broadening and instead strongly influence the domain structure at the SRT²⁷ in agreement with experiment.¹⁵ For the continuous transition via the canting of magnetization, the domain microstructure enables a continuous transition from a domain structure with vertical magnetization to a vortex structure for in-plane magnetization. For the discontinuous transition, a state of coexisting domains with vertical and in-plane magnetizations is found. The size of the vertical and the in-plane domains depends on the ratio of second- and fourth-order anisotropy and changes continuously throughout the SRT.²⁷

In an experiment, the ideal structure can hardly be realized. Ultrathin films frequently comprise a local varying thickness which further complicate the interpretation of magnetization behavior at the SRT measured by averaging methods. This fact stimulates the use of high resolution magnetic microscopy (e.g., SP-STM) with the aim of avoiding averaging of areas of different thicknesses. This study reports on the temperature-driven SRT in 1.5 ML Fe on Mo(110) from a vertical easy axis at 5 K to an in-plane direction at 20 K. For a comparison with theoretical models, the investigation of a temperature-driven SRT is particularly interesting because temperature is a free parameter that can be changed continuously and reversibly, in contrast to, e.g., the thickness.

Since the zero field configuration is of interest, we determine the magnetic contrast from the asymmetry of local conductivity for oppositely magnetized domains. As an approximation, we assume that the contrast is proportional to $\vec{m}_{\text{tip}} \cdot \vec{m}_{\text{sample}}$,²⁸ where \vec{m}_i denotes the magnetization of tip and sample, respectively. This proportionality only holds under special circumstances.²⁹ In general, the magnetic contrast depends on the applied bias voltage and on the absolute spin polarization of tip and sample. Moreover, when the integrated asymmetry of the tunneling current is not zero, an additional offset occurs in the dI/dU map due to a different tip-sample distance.²⁹ Therefore, we use tips of the same material for all measurements, and we applied the same bias voltage for both tips, providing almost zero net spin polar-

ization of the tunneling current. Hence, using tips with out-of-plane and in-plane sensitivities, two independent magnetization components were detected.

II. EXPERIMENT

The experiments were performed in a two-chamber UHV system, allowing an *in situ* sample or tip preparation and low-temperature scanning tunneling microscopy (STM) as described previously.³⁰ Sample cleanliness and surface structure were investigated by Auger electron spectroscopy and low energy electron diffraction. Low-temperature STM could be performed in zero field in a temperature range of 5–30 K. The temperature of the sample was measured using a Si diode with an accuracy of ± 0.25 K. The temperature had to be stabilized better than ± 1 K prior to tip approach using a manually controlled heating device.

Before the sample preparation, the Mo(110) substrate surface was cleaned using alternating cycles of annealing in oxygen (5×10^{-8} mbar) and flashing at 2000 K.³¹ Ultrathin Fe films of 1–2 ML thickness were evaporated on a Mo(110) surface in UHV (base pressure below 1×10^{-10} mbar) at a substrate temperature of 700 K. At this temperature, Fe mainly grows by step-flow growth forming alternating monolayer (ML) and double layer stripes.^{30,32–34}

For SP-STM, we have used tungsten tips flashed at 2200 K and subsequently covered by 10 ML Au and 4 (16) ML Co at room temperature.³¹ Due to the thickness-driven SRT of Co films on Au,^{17,35–37} tips with 4 ML Co show an out-of-plane and tips with 16 ML Co an in-plane magnetic sensitivity.³¹ STM images were measured in a constant current mode at a stabilizing current of 1.5 nA and sample bias of 0.3 V. For simultaneous measurement of differential conductance (dI/dU) maps using a lock-in technique, we added a modulation voltage with a frequency of 7 kHz and an amplitude of 30 mV to the sample bias. SP-STM was performed in runs with warming up and/or cooling down the sample within the totally available temperature range from 5 to 30 K.

III. RESULTS AND DISCUSSION

Figure 1(a) shows a topographic STM image ($500 \times 150 \text{ nm}^2$) of 1.5 ML Fe grown on Mo(110) at 700 K. Due to the step-flow growth mode, alternating Fe ML and DL stripes are formed.^{30,32–34} Topographical steps with a height of 10% of the atomic step height (0.2 nm) appear up at the boundary between ML and DL areas, indicating the steps of the substrate surface. We also observe dislocation lines on the DL stripes that are caused by the pseudomorphic strain (10%) according to previous observations.

Figure 1(b) shows the corresponding map of the local conductivity (dI/dU map), where a bright (dark) color indicates high (low) conductivity. Because the electronic structure of Fe ML and DL on Mo(110) is different, the dI/dU value of the ML is higher at a sample bias of 0.3 V and appears as a bright area in the dI/dU map.^{30,31} The DL areas instead appear darker and on top of that show two distinct values. This additional difference has a magnetic

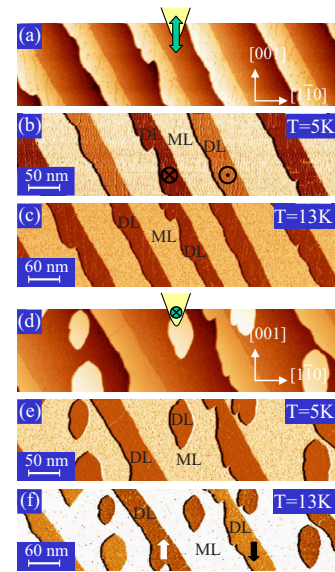


FIG. 1. (Color online) (a) Topographic STM image ($500 \times 150 \text{ nm}^2$), and (b) simultaneously measured differential conductance dI/dU map of 1.5 ML Fe grown on Mo(110) at 700 K taken at 5 K. (c) The dI/dU map measured for the same sample area as in (b) but taken at 13 K. Images (a)–(c) are obtained using the W/10 ML Au/4 ML Co magnetic tip of the out-of-plane magnetic sensitivity. (d) Topographic STM image ($500 \times 150 \text{ nm}^2$), and (e) simultaneously measured differential conductance dI/dU map of 1.5 ML Fe/Mo(110) nanostructures taken at 5 K by means of the W/10 ML Au/16 ML Co magnetic tip revealing the in-plane magnetic sensitivity. (f) The dI/dU map of the same sample position as in (e) and acquired with the same tip at 13 K. For comparison, the relative orientation of the DL Fe/Mo(110) nanowire magnetization is shown in (b) and (f).

origin.^{30,31,34} It results from the fact that the DL Fe wires are magnetized either “up” or “down” perpendicularly to the surface. The two distinct dI/dU values indicate a homogeneous magnetization within each nanostripe. The antiparallel orientation of the magnetization in adjacent stripes is the result of the dipolar antiferromagnetic coupling.

The magnetic contrast for the Fe DL stripes has disappeared at 13 K, as illustrated in Fig. 1(c). The dI/dU map in Fig. 1(c) was measured for the same sample position and with the same settings as in Fig. 1(a). It shows a slightly larger area due to the temperature dependence of the piezo-response of the scanner.

A similarly prepared sample was investigated using a magnetic tip with in-plane sensitivity (16 ML Co). The topography, shown in Fig. 1(d), comprises a few Fe DL islands in addition to the DL stripes. The islands nucleate because of the increased terrace width at this sample position. At 5 K, the Fe DL stripes do not reveal any in-plane magnetic contrast [Fig. 1(e)] as can be deduced from the homogeneous dI/dU value on the DL areas. After increasing the temperature to 13 K, we observe the onset of the in-plane magnetic contrast, as illustrated in Fig. 1(f). Fe DL stripes attached at adjacent substrate steps are magnetized oppositely to each other. The magnetization in the Fe DL islands shows parallel or antiparallel to the DL stripe on the same terrace. Accord-

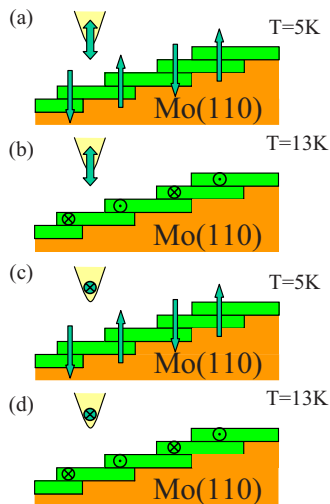


FIG. 2. (Color online) Schematic drawings illustrating the results presented in Fig. 1. The relative orientations of the DL Fe nanowires magnetization, and the directions of the magnetic sensitivity of the tips are shown for the different temperatures, for [(a) and (b)] the out-of-plane and [(c) and (d)] the in-plane magnetic sensitivities, respectively.

ing to the homogeneous dI/dU value measured on individual DL areas, the magnetization appears homogeneous in each stripe or island.

Figure 2 schematically shows the four nonequivalent cases of relative orientations of the Fe DL magnetization and the directions of the magnetic sensitivity of the tips at 5 and 13 K. A change of the magnetic contrast with increasing temperature can also be caused by a SRT of the tip magnetization instead of the sample magnetization. In the following, we argue why this is not the case. The previously studied magnetic phase diagram for the Co/Au/W system¹⁷ clearly indicates that the critical Co thickness of the SRT shifts toward larger film thickness with decreasing temperature. Below 100 K, a perpendicular orientation of magnetization is observed up to a 9 ML thick Co film,¹⁷ in agreement with our previous results.³¹ Therefore, the 4 ML Co film in our case certainly keeps the perpendicular sensitivity in the total temperature range of this experiment. If the easy axis of the in-plane sensitive tip with 16 ML Co had changed from in plane to perpendicular with decreasing temperature, we would have observed at 5 K a magnetic contrast in adjacent Fe DL stripes (which we never did) because the comparatively strong dipolar coupling assures antiparallel orientation in this case. On the other hand, if the magnetization in the Fe DL stripes had remained perpendicular independent of temperature, our measurements would have implied a magnetization rotation in the tip from in plane to out of plane with increasing temperature, which is rather unlikely and, moreover, in contradiction to the previously observed phase diagram.¹⁷ Consequently, a SRT of the magnetization in the Fe DL structures is the only remaining explanation.

The in-plane magnetization direction of the DL Fe stripes and islands could not be determined directly. The in-plane magnetization orientation of the tip is unknown. However, assuming a (110)-oriented tip apex, the residual epitaxial

strain in the Au buffer layer causes a uniaxial anisotropy in Co films on Au(111) on W(110).³⁶ Therefore, the in-plane sensitive tip will have a well-defined in-plane axis for each tip; however, its direction may assume a different in-plane angle after tip exchange.

The uniaxial anisotropy in Fe films on Mo(110) thicker than 2 ML shows along the in-plane [100] direction³⁸ at room temperature. We may assume here that the easy axis remains along this direction for thinner films and at lower temperatures. One should keep in mind that in-plane reorientation transitions can occur as, i.e., in the case of Fe/W(110) at 50 ML.³⁹

We never observed any magnetic contrast with both in-plane and out-of-plane sensitive tips on Fe ML regions for coverages larger than 1 ML. This fact has already been discussed for low-temperature (5 K) measurements.^{30,31} For submonolayer coverages, however, a pronounced magnetic contrast enabled the determination of the domain wall width in the Fe ML.^{30,31}

The magnetic contrast is specified by the asymmetry A of the conductivity signal, where we compare the cases of parallel and antiparallel alignments of the magnetizations of tip and sample:⁴⁰ $A = [dI/dU(\uparrow\uparrow) - dI/dU(\uparrow\downarrow)] / [dI/dU(\uparrow\uparrow) + dI/dU(\uparrow\downarrow)]$. At 5 K, we obtain $A_{\perp} = 30\%$ for the case of perpendicular magnetization in the Fe DL structures using W/Au/4 ML Co tips. At 13 K, the asymmetry has decreased to $A_{\perp} = 1\%$, while the in-plane asymmetry has increased to $A_{\parallel} = 2\%$.

For further investigation, we have performed measurements with out-of-plane and in-plane magnetic sensitive tips at different temperatures. Figure 3 shows a series of dI/dU maps acquired with an in-plane sensitive tip (16 ML Co) starting at 19 K [Figs. 3(b)] toward lower temperatures. The topography [Figs. 3(a)] slightly differs from the topography shown in Fig. 1(d), although the sample preparation parameters were nominally identical. Some of the DL Fe stripes are no longer continuous but show discontinuities. This might be caused by an increased contamination of the substrate during or before deposition. Abrupt switches of the DL magnetization to the opposite direction appear only at these discontinuities. This configuration is favorable because it completely avoids domain wall energy. A magnetization configuration, as shown in Fig. 3(b), of DL Fe stripes with switching magnetization along the stripes is exclusively observed for dominant in-plane magnetization. If out-of-plane magnetization is dominant, the dipolar coupling will force an antiparallel alignment of adjacent DL stripes.

The in-plane magnetic asymmetry measured at 19 K [Fig. 3(b)] is $A_{\parallel} = 30\%$. A_{\parallel} shows the same value as A_{\perp} at 5 K. Figures 3(c)–3(h) illustrate how the magnetic asymmetry evolves with decreasing temperature. The asymmetry decreases for lower temperatures and it is zero at 5.3 K.

Because the change of the sample temperature is always connected with an interruption of scanning, i.e., retracting and reapproaching of the STM tip, we occasionally observe a switch of the in-plane orientation of the tip magnetization. This switch is apparently caused by a magnetic (dipolar) sample or tip interaction during tip approach. Assuming a uniaxial anisotropy in the Co layer on the tip, the sample or tip interaction only leads to a reverse of the magnetic con-

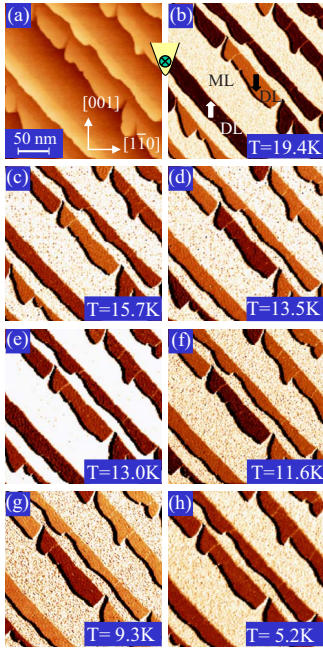


FIG. 3. (Color online) (a) Topographic STM image ($250 \times 250 \text{ nm}^2$), and (b) simultaneously measured differential conductance dI/dU map of 1.5 ML Fe grown on Mo(110) at 700 K taken at about 19 K. Arrows denote the DL Fe nanowires magnetization direction. [(c)–(h)] The dI/dU maps are taken at the different temperatures, as denoted, and measured at the same sample position as in (a) and (b). Presented images are obtained during the sample cooling using the W/10 ML Au/16 ML Co magnetic tip of the in-plane magnetic sensitivity. Note that near the transition temperature, a dramatic reduction of the magnetic contrast is observed (e). Occasionally, we see a flip of the tip magnetization as, e.g., from (c) to (d).

trast while the absolute value of A_{\parallel} remains the same. Interestingly, the smallest value of A is observed at the SRT (13 K) [Fig. 3(e)].

In the following, we compare the temperature dependence of A_{\perp} and A_{\parallel} as measured for a series with increasing and decreasing temperatures. Figure 4 shows the magnetic asymmetry of the DL Fe nanowires vs the sample temperature obtained with out-of-plane and in-plane sensitive tips and normalized to the value of the magnetic contrast A_i obtained in the first measurement at the lowest (highest) temperature in each run. The maximal asymmetries observed at the beginning of the runs are $A_{\perp}=30\%$ and $A_{\parallel}=30\%$, respectively.

At the lowest temperature (5 K), there is no in-plane asymmetry and the out-of-plane asymmetry achieves a maximum value, indicating vertical magnetization orientation in the Fe DL. In the temperature range between 5.5 and 13 K, we observe an increase of the in-plane contrast at the expense of out-of-plane asymmetry. This observation indicates that the magnetization in the Fe DL areas continuously rotates from perpendicular to in plane with increasing temperature. Above 15 K, the out-of-plane asymmetry remains zero, while the in-plane asymmetry further increased to a maximum value at 19 K. We observe a drop of both in-plane and out-of-plane contrasts close to zero at about 13 K, which

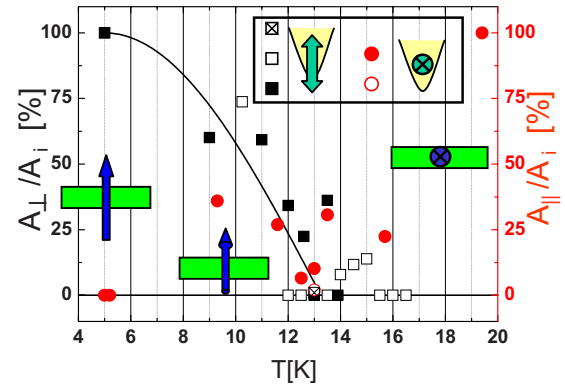


FIG. 4. (Color online) Magnetic contrast measured on the DL Fe nanowires vs the sample temperature for out-of-plane (squares) and in-plane (circles) magnetic sensitivities, respectively. The contrast is normalized to the A_i value obtained in the first measurement at the lowest (highest) temperature in each run. Open and closed symbols are measured in different series of experiments. The open and closed squares together with the open circles were measured with increasing temperature. The data denoted by closed circles and crossed squares are taken with decreasing temperatures. The magnetization direction is sketched for the different temperature regions.

cannot be explained by the simple models for the general behavior discussed below. As future experiments possibly will reveal, there may be interesting physics behind that.

Because the temperature sensor is not directly attached to the sample, there might be a deviation of a few Kelvins between the temperature reading and the actual temperature depending on the previous measurements in a series. This fact might explain the appearance of an out-of-plane asymmetry already at 15 K in the series of decreasing temperature [Fig. 4].

Assuming a magnetization rotation at the SRT in the plane that is expanded by the easy axis at 5 K, [110] (z axis), and the easy axis at 19 K, [001] (x axis), we would expect a temperature-independent absolute magnetization vector $m_0 = \sqrt{m_x^2 + m_z^2} = \sqrt{A_{\parallel}^2 + A_{\perp}^2}$. The small decrease of the magnetization due to the usual spin-wave excitation (Bloch law) can certainly be neglected in the narrow temperature range of the present investigation. An inspection of Fig. 4 shows that m is not constant at the SRT. Instead, we observe a strong decrease with a minimum at 13 K of about $m/m_0=0.04$.

This finding is in agreement with previous investigations of the SRT in Fe films. Strongly reduced out-of-plane and in-plane magnetization components were observed at the SRT for the systems Fe/Ag(100) (Refs. 41 and 42) and Fe/Cu(100).^{41,43} Instead of an intermediate paramagnetic state, this observation was later explained by pronounced domain formations.^{17,43} In contrast, for Co-based systems, the SRT could well be explained by a rotation of the magnetization vector with a constant absolute value.^{17,44–46} The occurrence of magnetic domains and, consequently, their responsibility for an apparent decreased magnetization value at the SRT can be excluded in our case.

We discuss three possible reasons for our observation of a decreased magnetization at the SRT. First, at the SRT, the

compensation of second-order magnetic anisotropies can destabilize magnetic order in two-dimensional systems. If no fourth-order anisotropies were present, the complete absence of anisotropy would lead to magnetic fluctuations near the SRT. Since SP-STM averages over the fluctuations in time, the result would be a decreased asymmetry at the SRT recovering at higher temperature because of the increasing in-plane anisotropy. However, in this case, one would expect a strong influence of finite-size effects for two-dimensional structures with lateral restrictions, which was never observed. Moreover, it is unlikely that the fourth-order anisotropy resulting from the bulk crystal anisotropy of Fe disappears.

Secondly, the assumption of a magnetization rotation in the x - z plane can be wrong. If, at the extreme, the magnetization shows along the $[1\bar{1}0]$ at the SRT, both components measured in the experiment will be zero. Therefore, a movement of the magnetization vector on a cone cannot be excluded. However, it is surprising that the sensitivity axis of our in-plane tip always remained in the same direction throughout all experiments.

The third reason is given by a mutual influence of the sample and tip magnetization caused by the dipolar interaction. This interaction will be particularly effective for in-plane sensitive tips because the in-plane anisotropy of the Co/Au/W(110) films on the tip apex is small. This fact causes the frequent contrast reversal observed in Fig. 3 and may also be responsible for the apparent drop of both in-plane and out-of-plane contrasts at the SRT.

IV. CONCLUSIONS

Using magnetic tips of in-plane and out-of-plane sensitivities, we observed a temperature-driven spin-reorientation transition in Fe DL nanostructures grown on Mo(110). At 5 K, the easy axis is perpendicular to the surface, while at 19 K, the easy axis is in plane presumably along $[001]$. The spin reorientation proceeds via magnetization canting as concluded from the simultaneous occurrence of in-plane and out-of-plane asymmetries at the same temperature. At the SRT (13 K), both in-plane and out-of-plane asymmetries are strongly decreased with respect to the expected value for a model of a rotating magnetization vector of constant length. We can rule out the formation of small magnetic domains at the SRT as a cause for this reduction. The reduction at the phase transition is most likely caused by mutual tip-sample interaction, but it can also indicate a rotation of the magnetization vector on a cone. Remarkable is the homogeneous asymmetry observed on the Fe DL structures independent of their shape and size. This indicates that the SRT is dominated by local magnetic anisotropies.

ACKNOWLEDGMENT

The financial support of the Deutsche Forschungsgemeinschaft (DFG) is gratefully acknowledged.

*Present address: Max-Planck Institut für Mikrostrukturphysik, Weinberg 2, 06120 Halle (Saale), Germany. jprokop@mpi-halle.mpg.de

¹U. Gradmann and J. Müller, Phys. Status Solidi **27**, 313 (1968).

²D. Sander, Rep. Prog. Phys. **62**, 809 (1999).

³M. Farle, Rep. Prog. Phys. **61**, 755 (1998).

⁴D. Sander, J. Phys.: Condens. Matter **16**, R603 (2004).

⁵P. J. Jensen and K. H. Bennemann, Surf. Sci. Rep. **61**, 129 (2006).

⁶*Ultrathin Magnetic Structures IV: Applications of Nanomagnetism*, edited by B. Heinrich and J. A. C. Bland (Springer-Verlag, Berlin, 2005).

⁷*Ultrathin Magnetic Structures III: Fundamentals of Nanomagnetism*, edited by J. A. C. Bland and B. Heinrich (Springer-Verlag, Berlin, 2005).

⁸H. J. Richter and S. D. Harkness IV, Mater. Res. Bull. **31**, 384 (2006).

⁹J. A. Katine, F. J. Albert, R. A. Buhrman, E. B. Myers, and D. C. Ralph, Phys. Rev. Lett. **84**, 3149 (2000).

¹⁰S. A. Wolf, D. Treger, and A. Chitchekanova, Mater. Res. Bull. **31**, 400 (2006).

¹¹M. Donath, J. Phys.: Condens. Matter **11**, 9421 (1999).

¹²R. Allenspach and A. Bischof, Phys. Rev. Lett. **69**, 3385 (1992).

¹³I.-G. Baek, H. G. Lee, H.-J. Kim, and E. Vescovo, Phys. Rev. B **67**, 075401 (2003).

¹⁴A. Dittschar, M. Zharnikov, W. Kuch, M.-T. Lin, C. M. Schneider, and J. Kirschner, Phys. Rev. B **57**, R3209 (1998).

¹⁵K. von Bergmann, M. Bode, and R. Wiesendanger, J. Magn. Magn. Mater. **305**, 279 (2006).

¹⁶D. P. Pappas, K.-P. Kamper, and H. Hopster, Phys. Rev. Lett. **64**, 3179 (1990).

¹⁷R. Sellmann, H. Fritzsche, H. Maletta, V. Leiner, and R. Siebrecht, Phys. Rev. B **64**, 054418 (2001).

¹⁸H. Fritzsche, J. Kohlhepp, H. J. Elmers, and U. Gradmann, Phys. Rev. B **49**, 15665 (1994).

¹⁹N. D. Mermin and H. Wagner, Phys. Rev. Lett. **17**, 1133 (1966).

²⁰M. Bander and D. L. Mills, Phys. Rev. B **38**, 12015 (1988).

²¹Y. Millev and J. Kirschner, Phys. Rev. B **54**, 4137 (1996).

²²H. P. Oepen, M. Speckmann, Y. T. Millev, and J. Kirschner, Phys. Rev. B **55**, 2752 (1997).

²³M. Speckmann, H. P. Oepen, and H. Ibach, Phys. Rev. Lett. **75**, 2035 (1995).

²⁴T. Duden and E. Bauer, Phys. Rev. Lett. **77**, 2308 (1996).

²⁵R. Zdyb and E. Bauer, Phys. Rev. B **67**, 134420 (2003).

²⁶E. Y. Vedmedenko, H. P. Oepen, A. Ghazali, J.-C. S. Levy, and J. Kirschner, Phys. Rev. Lett. **84**, 5884 (2000).

²⁷E. Y. Vedmedenko, H. P. Oepen, and J. Kirschner, Phys. Rev. B **66**, 214401 (2002).

²⁸A. Kubetzka, O. Pietzsch, M. Bode, R. Ravlić, and R. Wiesendanger, Acta Phys. Pol. A **104**, 259 (2003).

²⁹A. Kubetzka, O. Pietzsch, M. Bode, and R. Wiesendanger, Appl. Phys. A: Mater. Sci. Process. **76**, 873 (2003).

³⁰J. Prokop, A. Kukunin, and H. J. Elmers, Phys. Rev. Lett. **95**, 187202 (2005).

- ³¹J. Prokop, A. Kukunin, and H. J. Elmers, *Phys. Rev. B* **73**, 014428 (2006).
- ³²J. Malzbender, M. Przybylski, J. Giergiel, and J. Kirschner, *Surf. Sci.* **414**, 187 (1998).
- ³³S. Murphy, D. Mac Mathuna, G. Mariotto, and I. V. Shvets, *Phys. Rev. B* **66**, 195417 (2002).
- ³⁴M. Bode, O. Pietzsch, A. Kubetzka, and R. Wiesendanger, *Phys. Rev. Lett.* **92**, 067201 (2004).
- ³⁵R. Allenspach, M. Stampanoni, and A. Bischof, *Phys. Rev. Lett.* **65**, 3344 (1990).
- ³⁶T. Duden and E. Bauer, in *Magnetic Ultrathin Films, Multilayers and Surfaces*, MRS Symposia Proceedings No. 283 (Materials Research Society, Pittsburgh, 1997).
- ³⁷H. F. Ding, S. Pütter, H. P. Oepen, and J. Kirschner, *Phys. Rev. B* **63**, 134425 (2001).
- ³⁸V. Usov, S. Murphy, and I. V. Shvets, *J. Magn. Magn. Mater.* **283**, 357 (2004).
- ³⁹U. Gradmann and G. Waller, *Surf. Sci.* **116**, 539 (1982).
- ⁴⁰M. Bode, *Rep. Prog. Phys.* **66**, 523 (2003).
- ⁴¹D. P. Pappas, C. R. Brundle, and H. Hopster, *Phys. Rev. B* **45**, 8169 (1992).
- ⁴²Z. Q. Qiu, J. Pearson, and S. D. Bader, *Phys. Rev. Lett.* **70**, 1006 (1993).
- ⁴³R. Allenspach, *J. Magn. Magn. Mater.* **129**, 160 (1994).
- ⁴⁴C. Chappert and P. Bruno, *J. Appl. Phys.* **64**, 5736 (1988).
- ⁴⁵V. Grolier, J. Ferre, A. Maziewski, E. Stefanowicz, and D. Renard, *J. Appl. Phys.* **73**, 5939 (1993).
- ⁴⁶G. Garreau, E. Beaurepaire, K. Ounadjela, and M. Farle, *Phys. Rev. B* **53**, 1083 (1996).